SISSA

PAPER

A biased intruder in a dense quiescent medium: looking beyond the force–velocity relation

View the article online for updates and enhancements.

Related content

- Microrheology of colloidal systems
  A M Puertas and T Voigtmann

- Anomalous transport in the crowded world of biological cells
  Felix Höfling and Thomas Franosch

- Survival probability of an immobile target surrounded by mobile traps
  Jasper Franke and Satya N Majumdar

Recent citations

- Editorial: Anomalous Transport: Applications, Mathematical Perspectives, and Big Data
  Carlos Mejía-Monasterio *et al*

- Trace of anomalous diffusion in a biased quenched trap model
  Takuma Akimoto and Keiji Saito

- Active microrheology, Hall effect, and jamming in chiral fluids
  C. Reichhardt and C. J. O. Reichhardt

IOP ebooks™

Bringing together innovative digital publishing with leading authors from the global scientific community.

Start exploring the collection–download the first chapter of every title for free.

A biased intruder in a dense quiescent medium: looking beyond the force–velocity relation

Olivier Bénichou[1], Pierre Illien[1], Carlos Mejía-Monasterio[2,3] and Gleb Oshanin[1]

[1] Laboratoire de Physique Théorique de la Matière Condensée (UMR CNRS 7600), Université Pierre et Marie Curie (Paris 6), 4 Place Jussieu, F-75252 Paris, France
[2] Laboratory of Physical Properties, Technical University of Madrid, Avenida Complutense s/n, E-28040 Madrid, Spain
[3] Department of Mathematics and Statistics, University of Helsinki, PO Box 68, FI-00014 Helsinki, Finland
E-mail: benichou@lptmc.jussieu.fr, illien@lptmc.jussieu.fr, carlos.mejia@upm.es and oshanin@lptmc.jussieu.fr

Abstract. We study the dynamics of a biased intruder (BI) pulled by a constant force $\mathbf{F}$ through a dense molecular crowding environment modelled as a lattice gas of unbiased, randomly moving hard-core particles. Going beyond the usual analysis of the force–velocity relation (FVR), we focus on the behaviour of the higher moments of the BI vector displacement $\mathbf{R}_n$ at time n (the FVR is just the first moment) in the leading order in the density ρ_0 of vacancies ($\mathrm{O}(\rho_0)$). We prove that in infinite 2D systems the probability distribution $P(\mathbf{R}_n)$ converges to a Gaussian as $n \to \infty$, despite the fact that the BI drives the system into a non-equilibrium steady state with a non-homogeneous spatial distribution of the lattice gas particles. We show that in infinite 2D systems the variance σ_x^2 of the distribution $P(\mathbf{R}_n)$ along the direction of the bias grows (weakly) super-diffusively: $\sigma_x^2 \sim \nu_1\, n\, \ln(n)$. In the direction perpendicular to the bias, the variance $\sigma_y^2 \sim \nu_2\, n$. The coefficients ν_1 and ν_2, which we determine exactly for arbitrary bias in $\mathrm{O}(\rho_0)$, mirror the interplay between the bias, vacancy-controlled transport and the back-flow effects of the medium on the BI. We observe that $\nu_1 \sim |\mathbf{F}|^2$ for small bias, which signifies that the super-diffusive behaviour emerges beyond the linear-response approximation. We present analytical arguments

showing that such an anomalous, field-induced broadening of fluctuations is dramatically enhanced in confined, quasi-1D geometries—infinite 2D stripes and 3D capillaries. We argue that in such systems, σ_x^2 exhibits a strongly super-diffusive behaviour, $\sigma_x^2 \sim n^{3/2}$. Monte Carlo simulations confirm our analytical results.

Keywords: driven diffusive systems (theory), exact results, stochastic particle dynamics (theory), microfluidics

Contents

1. Introduction

A biased intruder (BI)—a particle which performs a random motion biased in one direction in a quiescent bath of other particles, which also move randomly but without any preferential direction—drives the spatial distribution out of equilibrium. The bath particles accumulate, creating a 'traffic jam' in front of the BI, and are depleted behind it. The BI can be, e.g., a charge carrier subject to an electric field or a colloid moved with an optical tweezer. The bath particles may be, e.g., colloids dispersed in a solvent or

entrapped by a liquid–liquid interface, or adatoms performing activated hopping motion among the adsorption sites on a solid surface.

Microstructural changes of the (otherwise homogeneous) medium have been observed experimentally. In particular, experiments revealed such changes in active microrheological measurements of the drag force exerted on a single colloid driven through a λ-DNA solution [1], for an intruder driven by a constant-velocity optical trap in a monodisperse quasi-two-dimensional colloid suspension [2] or for an intruder dragged through a monolayer of vibrated grains [3]. Formation of a non-homogeneous and non-equilibrium distribution of the bath particles has also been evidenced by Brownian dynamics simulations of a driven colloid in λ-DNA solutions [1, 4], in molecular dynamics simulations of a three-dimensional Lennard-Jones binary mixture [5] and in colloidal crystals [6]. In the latter case, it was shown that a large enough BI generates a stress sufficient to produce defects, which remain localized near the BI and affect the frictional drag force. The microstructural changes of the medium not only enhance the drag force exerted on the BI, but also induce effective interactions between the BIs, when more than one BI is present [7]–[11].

Microstructural changes of the medium manifest themselves via peculiar forms of the so-called force–velocity relation (FVR), i.e., the dependence of the terminal BI velocity v on the magnitude of the pulling force F. Such FVRs have been extensively studied in the past for various complex fluids such as glasses [12], colloidal systems [13, 14] and also granular media [3], [15]–[18]. The measured FVRs display several regimes with a linear Stokesian behaviour for sufficiently small forces or small packing fractions, and a non-linear behaviour close to the glass and/or jamming transition. Some theoretical results on out-of-equilibrium response functions and generalized fluctuation-dissipation relations for granular intruders can be found in the recent work [19]. We also note parenthetically that similar effects were predicted, in general, for driven inclusions which locally affect the fluctuations of thermally excited fields, inducing thermal Casimir drag forces acting on the inclusions and, hence, resulting in very special forms of the FVR (see, e.g., [20]–[22] and references therein).

Microstructural changes of the medium produced by a BI were extensively studied analytically for quiescent baths modelled as hard-core lattice gases with symmetric simple exclusion dynamics [23]–[29]. In this case, the intruder is absolutely identical to the bath particles, except that it is biased and thus has a preferential direction of motion. In this regard, one studies here the dynamics of an *asymmetric* simple exclusion process (ASEP) [30] in a d-dimensional sea of symmetric simple exclusion processes (SEPs) [31]. From a different perspective, one considers a theoretical model in a standard, probe-based, constant-forcing microrheological set-up. Despite some evident simplifications made in such a type of modelling, as well as in its subsequent generalizations over the lattice gases with kinetic constraints (i.e., it is assumed that the interactions are merely hard-core ones, with no rotational diffusion and no momentum transfer, the particles are constrained to move on a lattice, and so on), it captures quite well several essential qualitative features and reproduces, in some cases, a cooperative many-particle behaviour which is observed in realistic physical systems [31]–[42]. Some other examples that lattice gas modelling successfully explains include, e.g., the experimentally observed spreading behaviour of the so-called precursor films [43, 44], wetting/dewetting transitions of monolayers confined in

slit-like pores [45] and knot-limited polymer ejection from a capsid [46], to name just a few.

It was realized that in one-dimensional (1D) symmetric, hard-core lattice gases, i.e., in the so-called single-file systems, the size of the jammed region in front of the BI grows in proportion to the distance travelled. This means that the jamming-induced contribution to the frictional drag force exerted by the medium on the BI exhibits an unbounded growth with time n, so its mean displacement grows sub-linearly, in proportion to $\sqrt{n}$. In other words, the BI mean velocity v_n vanishes, $v_n \propto 1/\sqrt{n}$ [23]–[25]. This ensures the validity of the Einstein relation between the mobility and the diffusivity for anomalous tracer diffusion in 1D hard-core lattice gases [24]–[26], [47, 48], for which the variance σ_x^2 of the BI displacement in the absence of the bias grows sub-diffusively, according to the celebrated asymptotic law $\sigma_x^2 \sim \sqrt{n}$ [49]–[54]. Note, as well, that in the absence of an external pulling force, the distribution of the displacement of the (unbiased) intruder converges to a Gaussian [54]. The $\sigma_x^2 \sim \sqrt{n}$ law has also been observed experimentally (see, e.g., [55, 56]).

In higher dimensions the situation is qualitatively different: after some transient period of time, the BI starts to move ballistically, so its mean velocity approaches a terminal value v, which depends on the particle density ρ and on the value of the applied force. The FVR displays a linear, Stokesian behaviour for sufficiently small values of the pulling force, and the proportionality factor can be identified as an effective friction coefficient. The latter comprises a mean-field contribution (corresponding to perfectly mixed lattice gases) and an essentially cooperative contribution (associated with the microstructural changes of the medium). Furthermore, for biased dynamics in lattice gases the force–velocity curve saturates[4], i.e., the velocity attains some constant limiting value, when the force tends to infinity, so the intruder performs a unidirectional random motion [26, 28, 29]. In turn, the bath particle spatial distribution attains, in the frame of reference moving with the BI, a non-equilibrium stationary form characterized by a jammed region in front of the BI and a depleted region in its wake (see figure 1) [27]–[29]. Strikingly, behind the BI the bath particle density approaches the mean value ρ as a power law in the distance x: $1/x^{3/2}$ and $\ln(x)/x^2$ in 2D and 3D [27]–[29]. This signifies that the medium 'remembers' the passage of the BI on anomalously large temporal and spatial scales.

Given such an anisotropy in the bath particle spatial distribution and, in general, a non-equilibrium situation, quite a legitimate question to be addressed is that of a behaviour *beyond* the FVR: namely, of the time evolution of the higher moments of the BI displacement $\mathbf{R}_n$ at time n and, ideally, of the whole distribution $P(\mathbf{R}_n)$. Recall that the FVR is just the first moment of this distribution and, hence, does not provide all the wealth of information about the BI dynamics of course.

It has been recently discovered that the behaviour of the variance σ_x^2 of $\mathbf{R}_n$ along the direction of the applied bias (say, the x-direction) is, in fact, non-trivial and even counter-intuitive [57]–[61]. Dealing with such dense molecular crowding environments, one would expect to encounter a diffusive, or even a *sub-diffusive* behaviour. In contrast, it has been realized that the variance σ_x^2 along the direction of the bias exhibits a *super-diffusive* growth with time [57]–[61], in a striking contrast to the behaviour of either an

---

[4] Note that such a saturation stems from the definition of the microscopic dynamics of the intruder, in which the external bias enters via appropriately defined transition probabilities, normalized to unity. It may not be present in systems with other dynamic rules.
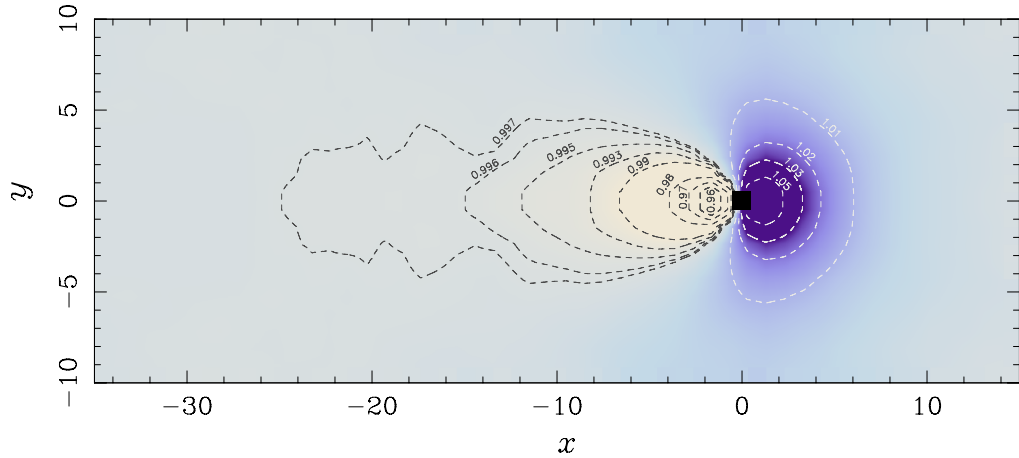
Figure 1. A snapshot of the bath particle density profile $\rho(x, y)$ relative to the mean density ρ (numbers near the contour curves) in a 2D hard-core lattice gas in the frame of reference moving with the BI (black square).

isolated biased Brownian particle or that of an unbiased diffusion in dense molecular crowding environments. In recent work [57]–[59], such an accelerated growth of σ_x^2 has been observed in molecular dynamics simulations of an intruder pulled by an external constant force through a glass-forming binary Yukawa fluid confined in an elongated (by the factor of 8 in the force direction) rectangular capillary $8L, L, L$, where $L = 13.3a$, a being the molecular diameter. It was realized that σ_x^2 grows with time n as $\sigma_x^2 \sim n^\xi$ with $\xi \approx 1.45$ [57, 58] or even $\xi \approx 1.5$ [59], with no apparent saturation of growth or crossover to diffusive behaviour at longer times. The variance in the direction perpendicular to the bias was shown to grow diffusively in the long-time limit. Furthermore, in a recent work [61], a non-linear transient regime[5], separating the initial and the ultimate diffusive behaviours with two different diffusion coefficients, has been observed in MD simulations of a binary mixture of Lennard-Jones particles, one of which was pulled by an external force, in a less elongated three-dimensional rectangular capillary with the aspect ratio 3:1:1[6].

Noticing a highly intermittent character of individual BI trajectories, such that the BI is localized for some time in a cage formed by the surrounding particles before it quickly moves to another cage, Winter *et al* [57, 58] argued that such an anomalous broadening of fluctuations in the dynamics of the pulled particle can be qualitatively understood in terms of a random trap model [62], since it is reminiscent of a directed walk among traps with a broad release time distribution. The authors, however, did not elaborate on this point and did not support it with any explicit calculation. Moreover, they observed in their numerical simulations that the release time, τ, distribution $\Psi(\tau)$ can be well-fitted by a stretched-exponential function, $\Psi(\tau) \sim \exp(-\sqrt{\tau})$, which seems, as a matter of fact, to be incompatible with their own claim, since such a distribution is not *broad*, possesses moments of arbitrary order and, hence, cannot be a cause of any anomalous behaviour. It was shown in [59] that a conventional mode-coupling-theory approach cannot reproduce such a super-diffusive behaviour either. A continuous-time random walk description (for

---

[5] See section 7 for a further discussion.
[6] We thank A Heuer for this clarification which was missing in the original [61].

5

general literature on the CTRW, see, e.g., [63]–[65]) of the dynamics of a biased intruder has been developed in [61], and the authors made a very strong claim that within a CTRW model an accelerated growth may take place at intermediate times, but ultimately it should cross over to a diffusive behaviour[7].

In our recent short paper [60], we studied analytically a BI dynamics in a molecular crowding environment modelled as a dense two-dimensional lattice gas of randomly moving hard-core particles, focusing on the question of how an asymmetry in the spatial distribution of the bath particles and, in general, a non-equilibrium situation affect the long-time evolution of the distribution $P(\mathbf{R}_n)$. We have shown, as a by-product of this analysis, that in the leading order in the density ρ_0 of vacancies, the variance of the BI displacement in the direction parallel to the bias exhibits an asymptotic (weakly) super-diffusive growth $\sigma_x^2 \sim n \ln(n)$ in *infinite* two-dimensional systems, and numerically observed a strongly super-diffusive growth, $\sigma_x^2 \sim n^{3/2}$, for *infinite* quasi-1D geometries— two-dimensional stripes and three-dimensional rectangular capillaries, which seems to be in a good agreement with the results of simulations in [57] for elongated 3D systems.

Taken together, the results of [57]–[59], [61] and of our work [60] hint at a possibility of encountering a novel phenomenon—a field-induced super-diffusive fluctuation broadening in the dynamics of a biased intruder moving in a quiescent medium, which goes beyond the usual FVR as well as such standard fluctuation-dissipation relations as the Green–Kubo or generalized Einstein relations [66, 67]. Some conflicting trends in the observed behaviour, however, call for a more thorough theoretical, numerical and experimental analysis with the goal of elucidating the physical mechanisms underlying such a phenomenon. Here we present an analytical analysis of this phenomenon in the case of a biased dynamics in lattice gases, which emphasizes the vacancy-controlled[8] mechanism of the super-diffusive fluctuation broadening, and the crucial importance of the effective spatial dimensionality and of the emerging long-range temporal correlations in the BI dynamics.

The purpose of the present paper is to give a complete and comprehensive discussion of a BI dynamics in very dense two-dimensional and several quasi-one-dimensional molecular crowding environments modelled as *lattice gases*, comprising hard-core particles which move randomly without any preferential direction. First of all, extending our succinct presentation in [60], we focus on the behaviour on infinite 2D lattices in the leading order in the density ρ_0 of vacancies (henceforth denoted as $\mathrm{O}(\rho_0)$). We determine exactly, in $\mathrm{O}(\rho_0)$ and for arbitrary bias F, the long-time behaviour of the variances, the skewness and the kurtoses of the probability distribution function $P(\mathbf{R}_n)$ of the BI vector displacement $\mathbf{R}_n$ at time n. We set out to show that the variance σ_x^2 along the direction of the bias exhibits a weakly super-diffusive growth, $\sigma_x^2 \sim \nu_1 n \ln(n)$, while the variance σ_y^2 in the direction perpendicular to the bias shows a usual diffusive growth, $\sigma_y^2 \sim \nu_2 n$. The coefficients ν_1 and ν_2, which result from the interplay between the bias, the vacancy-controlled transport, and the back-flow effects of the medium on the BI, are determined exactly, for arbitrary bias, in $\mathrm{O}(\rho_0)$. We realize that, remarkably, $\nu_1 \sim F^2$ for small pulling forces, which signifies that such a super-diffusive behaviour emerges beyond (and thus cannot be obtained within) the

---

[7] See, however, section 7 for a critical assessment of this claim and further discussion.

[8] Note that for the off-lattice systems studied in [57]–[59], [61], such a vacancy-facilitated motion of particles may take place only in a certain range of temperatures and densities, when the size of some elementary free-volume units or of some packing defects is comparable to that of the particles and so the latter may move diffusively by directly swapping their positions with the former [40, 68].

linear-response approximation. Furthermore, we show that the skewness of the distribution in the direction of the applied bias decays as $\sqrt{\ln(n)/n}$ and is positive, which means that fluctuations are more pronounced in the jammed region in front of the BI than in its wake, depleted by the gas particles. Next, we show that the kurtoses in both directions vanish in proportion to $\ln(n)/n$ and, hence, the probability distribution function $P(\mathbf{R}_n)$ of the BI vector displacement tends towards a Gaussian function as $n \to \infty$, at least for sufficiently dense systems, for both the direction perpendicular to the bias and that parallel to it. Note that the observation that the kurtosis of the distribution along the direction of the bias vanishes has also been made from numerical MD simulations in [61]. Clearly, when there is no external bias and the bath is homogeneous [54, 72], convergence of the distribution to a Gaussian one will not be a surprise. However, in our case, given a non-equilibrium situation and essential microstructural changes of the medium, this result certainly cannot be expected *a priori*.

Capitalizing on our results obtained via an exact approach, we present some phenomenological arguments which enable us to reproduce the dependence on n[9] of the variance σ_x^2 for infinite 2D systems in $\mathrm{O}(\rho_0)$ and to make predictions on the dynamical behaviour in other geometries. First, we argue that the same weakly super-diffusive behaviour $\sigma_x^2 \sim n \ln(n)$ as was observed for infinite strictly 2D systems should take place in infinite 3D slit-like pores (slabs) with finite width. Next, we argue that the super-diffusive broadening becomes much more pronounced in confined, quasi-1D geometries—infinite 2D stripes and 3D rectangular capillaries, in which the variance σ_x^2 of the distribution $P(\mathbf{R}_n)$ along the direction of the bias exhibits a strong power-law acceleration of growth, $\sigma_x^2 \sim n^{3/2}$ (compared to a diffusive growth $\sigma_x^2 \sim n$ in the absence of the bias). These results are supported by our numerical simulations. We note that the exponent '3/2' is specific to diffusive motion of vacancies; in the case where the particles (and hence, the vacancies) perform sub-diffusive motion, the exponent characterizing the growth of σ_x^2 will be higher.

In contrast, for strictly one-dimensional, single-file systems our simulations suggest that no *field-specific* behaviour takes place: we observe that the variance always goes as $\sigma_x^2 \sim \sqrt{n}$, as it does in the absence of any bias, and moreover, even the prefactor in this growth law is independent of the bias. These numerical results seem to be rather counter-intuitive, especially in view of a rather complicated form of the FVR for single-file systems [24]–[26]. This singular case will be examined analytically elsewhere [69]. Our results on the behaviour of the variance of the distribution along the direction of the bias are summarized in table 1.

Finally, noticing that in our lattice gas model the BI dynamics is also highly intermittent, we reconsider the CTRW-type picture presented in [61]. In contrast to [61], we do not resort to any *ad hoc* assumption on the form of the distribution of the key property in the CTRW picture—the discrete random process N_n describing the number of jumps made by the BI during time interval n. Our approach is based on the analysis of the microscopic dynamics. We show here that, in $\mathrm{O}(\rho_0)$, from the mathematical point of view the super-diffusive broadening of fluctuations in the confined geometries (stripes, capillaries, 2D systems and slabs, excluding the single files) arises due to the fact that the discrete random process N_n appears to be linked to a hidden random process, which behaves asymptotically as a super-diffusive fractional Brownian motion (fBm) [70] with

---

[9] Of course, using such qualitative arguments we cannot obtain the coefficients ν_1 and ν_2, as this requires a much more onerous analysis.

Table 1. The variance σ_x^2 of the distribution of the BI vector displacement at time n along the direction of the bias in O(ρ_0). Depending on the geometry of the system, the growth of σ_x^2 in this order can be sub-diffusive, diffusive or super-diffusive.

Geometry	Effective dimension	σ_x^2	Behaviour
Infinite 2D lattice	2D	$\sim n \ln(n)$	Weakly super-diffusive
Infinite 3D slit pore	Quasi-2D	$\sim n \ln(n)$	Weakly super-diffusive
Infinite 2D stripe	Quasi-1D	$\sim n^{3/2}$	Strongly super-diffusive
Infinite 3D capillary	Quasi-1D	$\sim n^{3/2}$	Strongly super-diffusive
Single file	1D	$\sim n^{1/2}$	Sub-diffusive
Infinite 3D lattice	3D	$\sim n$	Diffusive

positively correlated increments and which governs the long-time behaviour of the variance of N_n. From the physical point of view, the mechanism underlying this super-diffusive fBm-type process emerging in such confined geometries is associated with persistent recurrent returns to the BI location of the vacancies which have interacted once with the BI. Therefore, the BI dynamics represents a rather interesting combination of CTRW-type and fBm-type processes. This analysis confirms, also, our previous conclusion that no super-diffusive behaviour emerges in infinite three-dimensional systems.

This paper is structured as follows. In section 2 we describe the model and introduce basic notation. In section 3 we briefly outline the steps involved in the derivation of the propagator of a biased intruder in a two-dimensional lattice gas, infinite in both directions, with high particle density. Furthermore, in section 4, focusing on infinite two-dimensional square lattices, we present results exact in O(ρ_0) for the BI mean velocity (FVR), the variances, the skewness and the kurtoses of the probability distribution $P(\mathbf{R}_n)$ along the direction of the bias and in the direction perpendicular to it, as well as the results from the numerical Monte Carlo simulations. In section 5 we evaluate the leading long-time corrections to the asymptotic Gaussian forms of the distribution and compare them with the numerical data. In section 6 we present some qualitative theoretical arguments which support the time dependence of the variance σ_x^2 obtained in infinite 2D geometries in O(ρ_0) and allow us to make predictions for the behaviour in some confined geometries—infinite slit-like pores (slabs), two-dimensional stripes and three-dimensional capillaries—which have applications in microfluidics. Furthermore, we confirm our predictions by numerical simulations. In section 7 we revisit the phenomenological description based on a CTRW-like picture proposed in [61]. Finally, in section 8 we conclude with a brief recapitulation of our results.

2. The model and basic notation

We consider the dynamics of a BI on a square lattice of $L_x \times L_y$ sites $\mathbf{r} = (x, y)$ with integer valued components and periodic boundary conditions in both directions.

The lattice is populated with some amount of hard-core bath particles, placed at random subject to a single-occupancy condition, and a single hard-core intruder which is initially placed at the origin. M lattice sites are vacant and the initial positions of

the 'vacancies' are denoted by $\mathbf{Z}_0^j$, $j = 1, \ldots, M$. The system evolves in discrete time n and particles move randomly by exchanging their positions with the vacancies. The bath particles have symmetric hopping probabilities, i.e., given that a vacancy is at an adjacent site, any bath particle exchanges its position with the vacancy with probability $1/4$ independently of the direction. On the other hand, the intruder is subject to a constant force $\mathbf{F}$ orientated in the positive x-direction. The normalized jump probabilities of the (*isolated*) BI are given, in the usual fashion (see, e.g., [31]), by

$$p_\nu = \exp\left(\frac{\beta}{2}(\mathbf{F} \cdot \mathbf{e}_\nu)\right) \Big/ \sum_\mu \exp\left(\frac{\beta}{2}(\mathbf{F} \cdot \mathbf{e}_\mu)\right), \tag{1}$$

where β is the reciprocal temperature, $\mathbf{e}_\nu$ is the unit vector denoting the jump direction, $\nu \in \{\pm x, \pm y\}$, $(\mathbf{F} \cdot \mathbf{e}_\nu)$ is a scalar product and $\mathbf{F} = F\,\mathbf{e}_x$. The sum with the subscript μ (the normalization constant) denotes summation over all possible orientations of the vector $\mathbf{e}_\mu$.

We turn now to the limit of small density of vacancies, $\rho_0 = M/(L_x \times L_y) \ll 1$, and focus on the behaviour in $\mathrm{O}(\rho_0)$. Then, it is expedient to formulate the dynamics of the system in terms of the dynamics of vacancies. Following [72], we stipulate that at each tick of the clock each vacancy makes a step exchanging its position with a bath particle chosen at random (with probability $1/4$) from among its four neighbours, in the case when neither of them is the BI. If one of the neighbouring particles is the BI, the situation is a bit more complicated. According to [71] a correct choice of the transition probabilities, which avoids spurious temporal trapping, is as follows: if a vacancy is at site $\mathbf{R}_n + \mathbf{e}_\nu$ at time moment n and the BI occupies site $\mathbf{R}_n$, then it exchanges its position with the BI with probability

$$q_{-\nu} = \frac{p_\nu}{3/4 + p_\nu}, \tag{2}$$

and with the probability $1 - q_{-\nu} = 1/(3 + 4p_\nu)$ with any of three adjacent bath particles.

Note that in a complete description of the lattice gas dynamics, these rules would have to be supplemented for cases where two vacancies are adjacent or have common neighbours; however, these cases contribute only to $\mathcal{O}(\rho_0^2)$, so we can leave the rules for such events unstated in our theoretical analysis. For numerical simulations we use an obvious prescription: that when two (three, four) vacancies are adjacent or have common neighbours, a chosen vacancy attempting to make a move 'treats' the other vacancies as the bath particles. We note finally that analogous microscopic dynamic rules can be defined for any other above mentioned geometry.

The general properties of the BI dynamics that we are interested in here are the integrated distributions

$$P(X) = \sum_Y P(\mathbf{R}_n), \tag{3}$$

and

$$P(Y) = \sum_X P(\mathbf{R}_n), \tag{4}$$

along the direction of the bias and in the direction perpendicular to it, respectively, and their moments, such as the mean displacement $\overline{X}$ (and, hence, the mean velocity $v = \overline{X}/n$),

the variances σ_x^2 and σ_y^2, the skewness $\gamma_1(x)$ along the direction of the bias, and the kurtoses $\gamma_2(x)$ and $\gamma_2(y)$. The skewness is defined in the usual fashion as $\gamma_1(x) = k_3/\sigma_x^3$, where k_3 is the third cumulant of the distribution $P(X)$, while the kurtosis $\gamma_2(x)$ (or $\gamma_2(y)$) obeys $\gamma_2(x) = k_4/\sigma_x^4$ (or $\gamma_2(y) = k_4/\sigma_y^4$), where k_4 is the fourth cumulant of the distribution $P(X)$ $(P(Y))$.

3. The probability distribution in infinite 2D systems

Our analysis is based on the analytical approach developed previously by two of us for infinite two-dimensional lattices in [71], in which we extended to over a more general case of an intruder subject to an arbitrary constant force the seminal work by Brummelhuis and Hilhorst [72], who studied the dynamics of an unbiased intruder. In essence, this approach consists in assuming that the intruder encounters just a single vacancy at a time (which is appropriate at low density of vacancies in the system), so that the problem can be reduced to the description of interactions of the BI with just a single vacancy. The latter can be solved explicitly by representing the propagator of the BI at time n via recursion relations involving first-passage probabilities. This approach yields results which are *exact* in O(ρ_0) [72] and thus should be quite accurate when $\rho_0 \ll 1$. In what follows, we will check our analytical predictions against the results of numerical simulations for different densities of vacancies.

Here we briefly outline the main steps involved in the derivation of the probability distribution function of the BI vector displacement at time moment n. More details can be found in [71, 72]. Let $P(\mathbf{R}_n|\{\mathbf{Z}^j\})$ denote the probability of finding the BI at position $\mathbf{R}_n$ at time moment n as a result of its interaction with all the vacancies collectively,

$$P(\mathbf{R}_n|\{\mathbf{Z}^j\}) = \sum_{\mathbf{R}_n^1} \cdots \sum_{\mathbf{R}_n^M} \delta\left(\mathbf{R}_n, \mathbf{R}_n^1 + \cdots + \mathbf{R}_n^M\right) P(\mathbf{R}_n^1, \ldots, \mathbf{R}_n^M|\{\mathbf{Z}^j\}), \tag{5}$$

where $P_n(\mathbf{R}_n^1, \ldots, \mathbf{R}_n^M|\{\mathbf{Z}^j\})$ stands for the conditional probability that within the time interval n the BI has performed a displacement $\mathbf{R}_n^1$ due to the interactions with the first vacancy, a displacement $\mathbf{R}_n^2$ due to the interactions with the second vacancy, etc. In the lowest order in ρ_0, the vacancies contribute independently to the total BI displacement, so the latter conditional probability can be approximated as

$$P(\mathbf{R}_n^1, \ldots, \mathbf{R}_n^M|\{\mathbf{Z}^j\}) \simeq \prod_{j=1}^M P(\mathbf{R}_n|\mathbf{Z}^j), \tag{6}$$

where $P(\mathbf{R}_n|\mathbf{Z}^j)$ denotes the solution of a problem with only a single vacancy initially at $\mathbf{Z}_0^j$. Next, averaging $P(\mathbf{R}_n|\{\mathbf{Z}^j\})$ over the initial distribution of the vacancies, one finds [72]

$$P(\mathbf{R}_n) = \langle P(\mathbf{R}_n|\{\mathbf{Z}^j\})\rangle \simeq \sum_{\mathbf{R}_n^1} \cdots \sum_{\mathbf{R}_n^M} \delta\left(\mathbf{R}_n, \mathbf{R}_n^1 + \cdots + \mathbf{R}_n^M\right) \prod_{j=1}^M \langle P(\mathbf{R}_n|\mathbf{Z}^j)\rangle. \tag{7}$$

Furthermore, defining the Fourier transformed distributions

$$P_n(\mathbf{k}) = \sum_{\mathbf{R}_n} \exp\left(i(\mathbf{k}\cdot\mathbf{R}_n)\right) \langle P(\mathbf{R}_n|\{\mathbf{Z}^j\})\rangle, \tag{8}$$

and

$$p_n(\mathbf{k}) = \sum_{\mathbf{R}_n} \exp\left(\mathrm{i}(\mathbf{k} \cdot \mathbf{R}_n)\right) \left\langle P(\mathbf{R}_n|\mathbf{Z}^j) \right\rangle, \tag{9}$$

and summing over $\mathbf{R}_n$, one finds that

$$P_n(\mathbf{k}) \simeq p_n^M(\mathbf{k}), \tag{10}$$

which yields, upon going to the thermodynamic limit $L_x, L_y \to \infty$ (with $\rho_0 = M/(L_x \times L_y)$ and n kept fixed), the following general result:

$$P_n(\mathbf{k}) \simeq \exp\left(-\rho_0\, \Omega_n(\mathbf{k})\right). \tag{11}$$

Then, the desired probability distribution function obeys

$$P(\mathbf{R}_n) \simeq \frac{1}{4\pi^2} \int_{-\pi}^{\pi} \mathrm{d}\mathbf{k}\, \exp\left(-\mathrm{i}\,(\mathbf{k} \cdot \mathbf{R}_n) - \rho_0\, \Omega_n(\mathbf{k})\right). \tag{12}$$

Here $\Omega_n(\mathbf{k})$ is defined by

$$\Omega_n(\mathbf{k}) = \sum_{l=0}^{n} \sum_{\nu} \Delta_{n-l}(\mathbf{k}|\mathbf{e}_\nu) \sum_{\mathbf{Z} \neq 0} F_l^*(\mathbf{0}|\mathbf{e}_\nu|\mathbf{Z}), \tag{13}$$

where $F_l^*(\mathbf{0}|\mathbf{e}_\nu|\mathbf{Z})$ is the conditional probability for a random walk starting at $\mathbf{Z}$ to arrive for the first time at the origin at the nth step, being at site $\mathbf{0} + \mathbf{e}_\nu$ at time moment $n-1$ (see [71] for more details), and

$$\Delta_l(\mathbf{k}|\mathbf{e}_\nu) = 1 - p_l(\mathbf{k}) \exp\left(\mathrm{i}(\mathbf{k} \cdot \mathbf{e}_\nu)\right). \tag{14}$$

The function $\Omega_n(\mathbf{k})$ can be determined by introducing the generating function

$$\Omega_z(\mathbf{k}) = \sum_{n=0}^{\infty} \Omega_n(\mathbf{k})\, z^n, \tag{15}$$

for which one finds the following asymptotic solution [60]:

$$\Omega_z(\mathbf{k}) \underset{z \to 1^-}{\sim} \frac{1}{1-z} \frac{\Phi(\mathbf{k})}{1 - z + \chi_z^{-1}\Phi(\mathbf{k})}, \tag{16}$$

where

$$\chi_z \underset{z \to 1^-}{\sim} -\frac{\pi}{(1-z)\ln(1-z)}, \tag{17}$$

is the leading asymptotic term of the generating function of the *mean* number of 'new' (also called 'virgin' [65]) sites visited in the nth step.

Finally, the function $\Phi(\mathbf{k})$ obeys

$$\Phi(\mathbf{k}) = -\mathrm{i}a_0 k_x + \frac{a_1 k_x^2}{2} + \frac{a_2 k_y^2}{2}, \tag{18}$$

with $a_j = a_j(F)$ defined for arbitrary βF by

$$a_0 = \frac{\sinh(\beta F/2)}{(2\pi - 3)\cosh(\beta F/2) + 1}, \tag{19}$$

$$a_1 = \frac{\cosh(\beta F/2)}{(2\pi - 3)\cosh(\beta F/2) + 1},\tag{20}$$

and

$$a_2 = \frac{1}{\cosh(\beta F/2) + 2\pi - 3}.\tag{21}$$

Note that $P(\mathbf{R}_n)$ in equation (12) is normalized.

4. The FVR, the variances, the skewness and the kurtosis of the distribution for infinite 2D systems

4.1. The force–velocity relation

Differentiating the characteristic function $P_n(\mathbf{k})$ in equation (11) with respect to k_x and setting k_x and k_y equal to zero, one finds the following FVR:

$$v \sim \rho_0 \, a_0,\tag{22}$$

where the symbol '$\sim$' will denote from now on the exact (for arbitrary bias) leading large-n behaviour in $\mathrm{O}(\rho_0)$. Note that for $\beta F \ll 1$, equation (22) predicts a Stokesian, linear dependence of the velocity v on the magnitude of the applied bias F,

$$v \sim \frac{\beta \rho_0}{4(\pi - 1)} \, F,\tag{23}$$

in which $\zeta = 4(\pi - 1)/\beta\rho_0$ can be identified as the *friction* coefficient. Since the diffusion coefficient D of the intruder in the absence of the external bias is given in $\mathrm{O}(\rho_0)$ by $D = \rho_0/4(\pi - 1)$ (see, e.g., [32], [72]–[74] and references therein) one may immediately notice that:

- the result in equation (23) ensures the validity of the Einstein relation $\mu = \beta D$ between the diffusion coefficient and the mobility $\mu = \lim_{F\to 0} v/F$.

  Within the opposite limit $\beta F \gg 1$, the velocity saturates at a limiting value

$$v_\infty \sim \frac{\rho_0}{2\pi - 3}.\tag{24}$$

We hasten to repeat that such a saturation stems from the microscopic dynamic rules defined in our model and may not take place for systems in which the motion of the particles proceeds in a different way.

4.2. The variances

Furthermore, differentiating the characteristic function in equation (11) twice with respect to k_y (or k_x) and setting k_x and k_y equal to zero, we find the following asymptotic results for the variances of the distribution along the y- and x-axes

$$\sigma_y^2 \sim \rho_0 \, a_2 \, n\tag{25}$$

and

$$\sigma_x^2 \sim \rho_0 \left(a_1 + \frac{2a_0^2}{\pi} \left(H_{n+1} - 1 \right) \right) n,\tag{26}$$

where $H_n = \sum_{k=1}^{n} k^{-1}$ is the nth harmonic number.
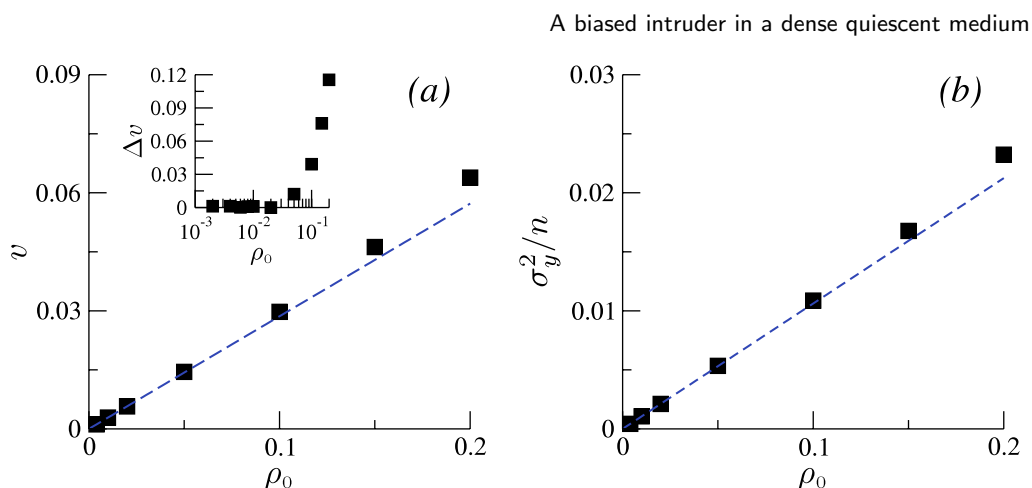
Figure 2. Velocity v (panel a) and σ_y^2/n (panel b) versus ρ_0 for $\beta F = 5$. The dashed lines define our theoretical predictions in equations (22) and (25), respectively. The inset in panel a shows the relative deviation of v from equation (22): $\Delta v = |v - \rho_0 a_0|/\rho_0 a_0$. The symbols here and henceforth denote the results of the numerical Monte Carlo simulations.

In figure 2 (panels a and b) we compare our analytical results for the mean velocity and the variance in the y-direction obtained in $\mathrm{O}(\rho_0)$ with the results of numerical simulations for fixed bias $\beta F = 5$ and different values of ρ_0. One notices that our analytical results are in very good agreement with the numerical data for ρ_0 up to 0.15.

Noticing next that in the large-n limit, $H_{n+1} \sim \ln(n) + \gamma + \mathcal{O}(1/n)$, where $\gamma \approx 0.577$ is the Euler–Mascheroni constant, we find that asymptotically

$$\sigma_x^2 \sim \rho_0 \left(a_1 + \frac{2a_0^2}{\pi} \left(\gamma - 1 \right) + \frac{2a_0^2}{\pi} \ln(n) \right) n. \tag{27}$$

On comparing the results in equations (25) and (27), we make two important observations:

- For a finite bias, the variance of the distribution along the x-axis grows (weakly) super-diffusively, due to an additional logarithmic factor, as compared to the variance along the y-axis, which shows a usual diffusive behaviour. Therefore, the distribution becomes progressively broader along the x-direction, as compared to its behaviour along the y-direction.
- The prefactor in the term proportional to $n \ln(n)$ in equation (27), i.e., $a_0^2 = v^2/\rho_0^2$, is proportional to $(\beta F)^2$ when $\beta F \ll 1$. This implies that such a super-diffusive behaviour emerges *beyond* and, hence, cannot be obtained *within* the linear-response approximation.

In figure 3 we present the evidence for the additional logarithmic factor in the x-component of the variance. Note parenthetically that such logarithmic corrections, which are specific to *infinitely* large systems, are notoriously difficult to observe. In our case, care has to be exercised to ensure that the BI and the vacancies (which, as a matter of fact, effectively move much faster than the BI) do not feel the finite-size effects, but also that, because of the periodic boundary conditions, there is no interference between the jammed region in front of the BI and the power-law wake depleted by the particles, which emerges behind the biased intruder. Moreover, since the logarithm is a slowly
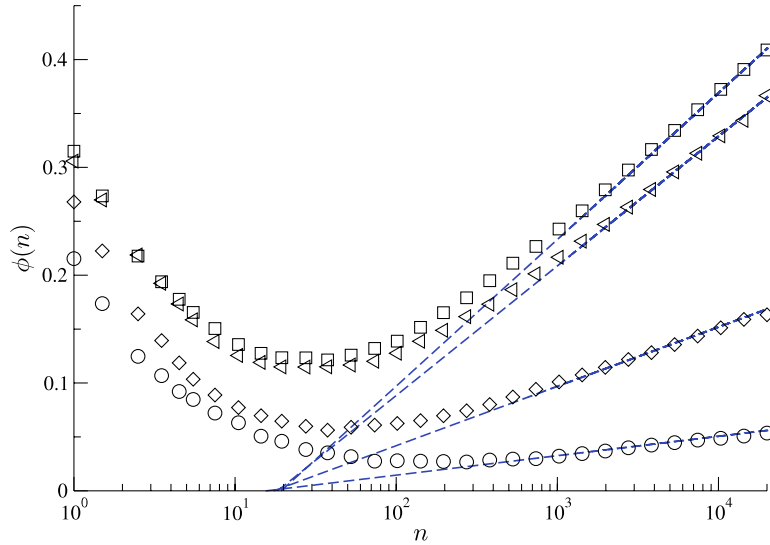
Figure 3. Numerical evidence for the logarithmic factor in σ_x^2. We plot $\phi(n)$ (see the text) versus $\ln(n)$ for $\rho_0 = 0.002$, $\beta F = 100$ ($\square$), $\beta F = 5$ ($\triangleleft$), $\beta F = 2$ ($\diamond$) and $\beta F = 1$ ($\circ$). The dashed lines are our predictions from equation (27).

varying function, one needs at least several decades of the observation time to confirm the logarithmic correction. To this end, in our numerical simulations we considered fairly large and elongated, dense lattice systems with $L_x = 5000$ and $L_y = 200$ and went to times of order 2×10^4. Next, to single out this contribution, we plotted here versus $\ln(n)$ the function $\phi(n) = \sigma_x^2/n - \rho_0(a_1 + 2a_0^2(\gamma - 1)/\pi)$, which according to our equation (27) should grow in proportion to $\ln(n)$. One does indeed observe an apparent crossover to a logarithmic behaviour, which persists then over two time decades.

It is important to remark that our numerical data (see figure 3) suggest that the crossover to an anomalous behaviour occurs quite early, at a time of the order of 10^3 steps. As a matter of fact, at such times the BI does not displace itself at any significant distance; on the contrary, for $\beta F = 1, 2, 5$ and 100, the average displacement amounts just to $0.2, 0.4, 0.56$ and 0.6 lattice spacings for $\rho_0 = 0.002$. This signifies that such a weakly super-diffusive behaviour can be accessed, in principle, by molecular dynamics simulations of off-lattice systems under appropriate density/temperature conditions.

4.3. The skewness and the kurtoses of the distribution

We note that the 'diffusive' growth of σ_y^2 does not ensure the convergence of the y-component of the distribution $P(\mathbf{R}_n)$ to the Gaussian distribution, and neither does the (weakly) super-diffusive growth of σ_x^2 rule out a long-time Gaussian behaviour of the x-component of the distribution $P(\mathbf{R}_n)$. To answer the question of the actual asymptotic behaviour of the propagator, we turn to the analysis of the higher moments of the distribution. It is straightforward to find that the asymptotic behaviour of the skewness $\gamma_1(x)$ of the distribution along the x-axis is given by

$$\gamma_1(x) \sim \frac{6a_0 \left(a_0^2 + \pi a_1/\ln(n)\right)}{\left(2a_0^2 + \pi a_1/\ln(n)\right)^{3/2}} \sqrt{\frac{\ln(n)}{\pi \rho_0 \, n}}. \tag{28}$$

Note that $\gamma_1(x) > 0$, so the distribution has a *positive* skew which implies that, rather counter-intuitively, fluctuations in the BI position are more pronounced for $X > v\,n$, i.e., in the region where the bath particles jam, than for $X < v\,n$, where the bath particles are essentially depleted. The skewness decays as $\gamma_1(x) \propto \sqrt{\ln(n)/n}$, i.e., somewhat more slowly, due to an additional factor $\sqrt{\ln(n)}$, than the skewness of the distribution in the case of an *isolated* biased particle.

Next, for the kurtosis $\gamma_2(x)$ we get

$$\gamma_2(x) \sim \frac{6 \left(4a_0^4 + 6a_0^2 \pi a_1 / \ln(n) + \pi^2 a_1^2 / \ln^2(n)\right)}{\left(2a_0^2 + \pi a_1 / \ln(n)\right)^2} \frac{\ln(n)}{\pi \rho_0 \, n}. \tag{29}$$

Conceptually this is a very important result because it shows that, at least in the lowest order in ρ_0, the kurtosis vanishes as $n \to \infty$, and, hence, that $P(X)$ *converges* to a Gaussian, despite a non-equilibrium situation and essential microstructural changes of the medium. Similarly to the skewness, the decay of the kurtosis again proceeds more slowly than in the case of an isolated biased particle due to an additional logarithmic factor.

Furthermore, we find that the third cumulant of the y-component of the distribution $P(\mathbf{R}_n)$ vanishes, and, hence, so does the skewness $\gamma_1(y)$, as it should. For the kurtosis of $P(Y)$ we obtain

$$\gamma_2(y) \sim \frac{6 \ln(n)}{\pi \, \rho_0 \, n}. \tag{30}$$

Curiously enough, the latter equation shows that $\gamma_2(y)$ asymptotically decays exactly in the same way as $\gamma_2(x)$, despite the fact that x- and y-directions are not equivalent because of the presence of a bias. Moreover, we observe that $\gamma_2(y)/\gamma_2(x) \to 1^-$ as $n \to \infty$, which means that at sufficiently large times the kurtoses in the x- and y-directions become equal to each other. Quite surprisingly,

- $\gamma_2(y)$ appears to be *independent* of the bias for the whole range of applicability of the result in equation (16),
- $\gamma_1(x)$ and $\gamma_2(x)$ become *independent* of the applied bias when $\ln(n) \gg \pi a_1$.

In contrast, the variances σ_x^2 and σ_y^2 do depend on βF.

We also note here parenthetically that for an *isolated* particle performing a biased Polya random walk, the distribution has a *negative* skew, the x- and y-components of both the skewness and the kurtosis are different, and, moreover, the x-components are strongly increasing functions of βF. Therefore, it is the perturbed quiescent medium which dictates this peculiar form of the distribution and damps down the dependence of $\gamma_1(x)$ and $\gamma_2(x)$ on βF.

In figure 4 (panels (a) and (b)) we compare our analytical predictions for $\gamma_1(x)$ and $\gamma_2(x)$ in equations (28) and (29) with the results of numerical simulations (symbols). To single out the logarithmic factors, we plot here the functions $\tilde{\gamma}_1(x) = n\,\gamma_1^2(x)$ and $\tilde{\gamma}_2(x) = n\gamma_2(x)$ versus $\ln(n)$. Note that the kurtosis approaches the asymptotic prediction in equation (29) quite rapidly, at times of order $n \sim 10^2$ and, moreover, the behaviour independent of βF is established quite fast as well. This confirms our result for the kurtosis and, hence, signifies that the distribution in the direction of the bias does indeed converge to a Gaussian. The skewness, which decays at a slower rate, approaches the asymptotic
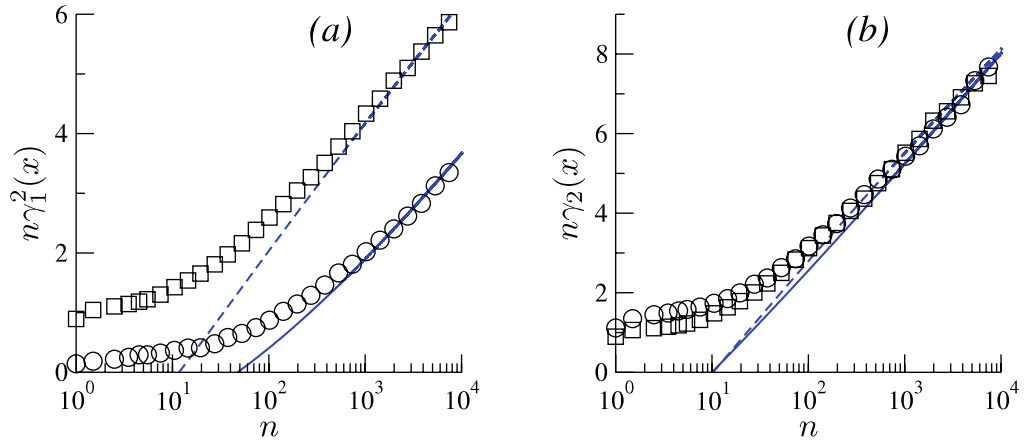
Figure 4. Reduced skewness $\tilde{\gamma}_1(x) = n\,\gamma_1^2(x)$ (panel (a)) and the kurtosis $\tilde{\gamma}_2(x) = n\gamma_2(x)$ (panel (b)) for $\rho = 0.002$, $\beta F = 1$ ($\circ$) and $\beta F = 100$ ($\square$). Dashed and solid lines are the corresponding theoretical results from equations (28) and (29).

result in equation (28) a decade later and the behaviour independent of βF sets in at larger times, which are not accessible in our numerical simulations of this essentially many-particle system.

5. Long-time corrections to the asymptotic Gaussian distribution in infinite 2D systems

We turn next to the corrections for large (but finite) n to the asymptotic Gaussian distribution of the BI position. For simplicity, we will not consider the complete distribution, but rather the behaviour of its components, equations (3) and (4). Multiplying both the numerator and the denominator of equation (16) by the complex conjugate of the denominator, introducing a small parameter $\epsilon_x = a_1 \ln(n)/2\pi\sigma_x^2 \propto 1/n$ and expanding $P_n(k_x, k_y = 0)$ in equation (11) up to the second order in ϵ_x, for the x-component of the distribution function we get

$$
P(X) = \frac{\exp\left(-\left(\eta_x - \overline{\eta}_x\right)^2/2\right)}{\sqrt{2\pi\sigma_x^2}}\{1 + [3(g-f) + 6f\overline{\eta}_x^2 - (g+f)\,\overline{\eta}_x^4
$$
$$
+ 2\left(3\left(g-2f\right) + (g+2f)\,\overline{\eta}_x^2\right)\overline{\eta}_x\,\eta_x - 6\left(g-f+f\overline{\eta}_x^2\right)\eta_x^2
$$
$$
- 2(g-2f)\,\overline{\eta}_x\,\eta_x^3 + (g-f)\,\eta_x^4]\,\epsilon_x + \mathcal{O}(\epsilon_x^2 \ln(n))\}, \tag{31}
$$

where we have conveniently chosen $\eta_x = X/\sigma_x$, $\overline{\eta}_x = vn/\sigma_x$, $g = 1 + a_0^2 \ln(n)/\pi a_1$ and $f = \pi a_1/2(\pi a_1 + 2a_0^2 \ln(n))$. In a similar fashion, introducing a small parameter $\epsilon_y = a_2 \ln(n)/2\pi\sigma_y^2 \propto \ln(n)/n$ and expanding $P_n(k_x = 0, k_y)$ in equation (11) up to the second order in ϵ_y, we obtain the following result for the y-component of the distribution:

$$
P(Y) = \frac{\exp\left(-\eta_y^2/2\right)}{\sqrt{2\pi\sigma_y^2}}\left\{1 + \left[3 - 6\eta_y^2 + \eta_y^4\right]\,\frac{\epsilon_y}{2} + \mathcal{O}(\epsilon_y^2)\right\}, \tag{32}
$$

16
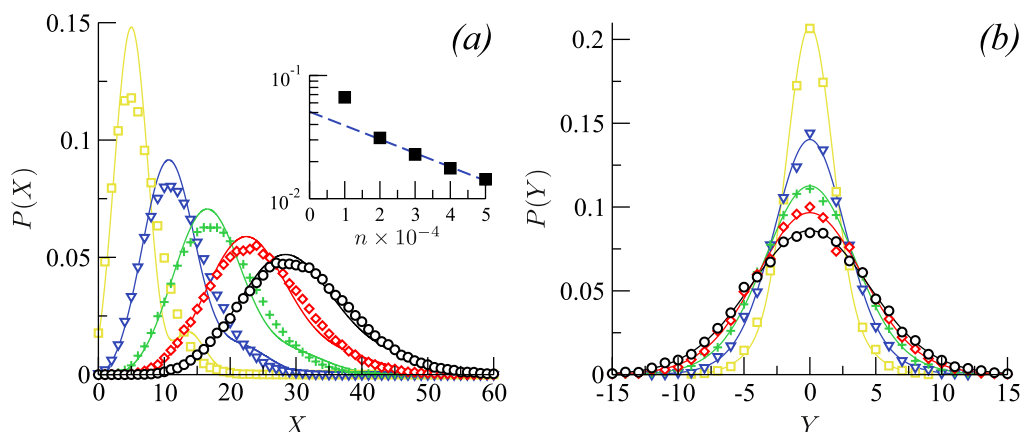
Figure 5. Time evolution of the x- and y-components of $P(\mathbf{R}_n)$ for times $n = 10^4$ (□), 2×10^4 (▽), 3×10^4 (+), 4×10^4 (◇) and 5×10^5 (○). The solid lines correspond to our results in equations (31) and (32). Panel (a): $P(X)$ for $\rho_0 = 0.002$ and $\beta F = 100$. The inset shows the L^2-distance between equation (31) and the numerical results (symbols). Panel (b): $P(Y)$ for $\rho_0 = 0.002$ and $\beta F = 1$.

where we have used the notation $\eta_y = Y/\sigma_y$. Note that equations (31) and (32) become identical when $\beta F = 0$.

In figure 5 (panels a and b) we compare the results from equations (31) and (32) against the numerical simulations data. We observe that as time progresses, the discrepancy between our equation (31) and the numerically obtained $P(X)$ gets smaller, as evidenced by the exponential decay of their L^2-distance (inset in panel a). However, it is worthwhile to remark that the convergence is non-uniform, so we have a better agreement between the theory and numerics for the values of X to the left from the maximum than to the right of it (recall that the distribution has a positive skew). In the direction perpendicular to the bias (panel b), we observe a pretty good agreement between our equation (32) and the numerical data.

6. Confined geometries: single files, slit pores, stripes and capillaries

We begin this section with the following remark: the appearance of the additional logarithmic factor in equation (27) in a two-dimensional infinite system under study can be interpreted as a sign that $d = 2$ is the *marginal* dimension for this problem, which is apparently associated with the fact that 2D is the marginal dimension in which random walks executed by the vacancies are recurrent. If this is true, one may expect that in three dimensions the variance will show a usual diffusive growth (with, however, a larger prefactor in the direction of the bias than in the direction perpendicular to it), and that in one-dimensional systems an additional power-law factor may emerge. Below, we analyse this question in detail.

6.1. Single-file systems

If the recurrence is the only criterion, we may expect the broadening effect to become much more pronounced for a biased diffusion in single-file systems, so the variance of
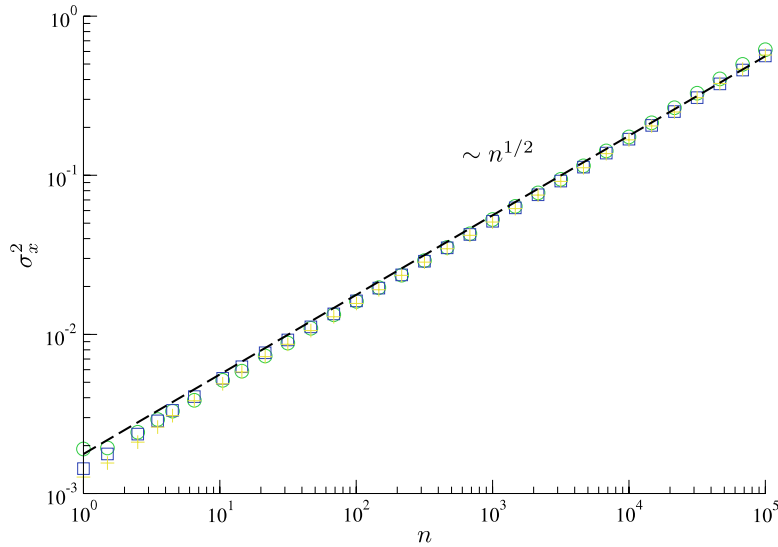
Figure 6. The variance σ_x^2 of the displacement of a biased intruder in dense (with $\rho_0 = 0.002$) single-file lattice gases for different values of βF: $\beta F = 1$ (○), $\beta F = 5$ (□) and $\beta F = 100$ (+). The dashed line indicates the slope $n^{1/2}$.

the biased intruder should get an additional power-law dependence in time. On the other hand, as we have already mentioned in section 1, single-file systems show a very singular, sub-diffusive behaviour in the absence of the bias [49]–[54] and a sub-linear growth of the mean displacement of a biased intruder [23]–[25], which is due to the fact that the particles cannot bypass each other. The outcome of the combined effect of these two competing factors is not clear *a priori*. Note, as well, that the theoretical analysis developed in the previous sections does not directly apply to single-file systems and here we resort instead to numerical analysis of the BI dynamics in dense single-file lattice gases of hard-core particles, looking beyond the force–velocity relation [24, 25]. Analytical analysis of the behaviour in single-file systems, which involves completely different physical mechanisms as compared to those for geometries with $d > 1$, will be presented elsewhere [69].

In figures 6 and 7 we present the results of the numerical simulations for the variance, skewness and kurtosis of the displacement of a biased intruder in single-file lattice gases. Observe that:

- the variance $\sigma_x^2 \sim n^{1/2}$, precisely as in the unbiased case, and moreover, even the prefactor appears to be *independent* of the value of the pulling force (as evidenced in figure 6);

- the skewness and the kurtosis decay as $1/n^{1/4}$ and $1/n^{1/2}$, respectively.

The skewness shows some variation with βF (notice that the curve for the smallest force $\beta F = 1$ goes apart of the curves for higher βF, which merge together) while the analogous dependence of the kurtosis is damped down completely. Therefore, we conclude that an external bias has almost no effect on the fluctuations of the BI dynamics in dense single-file lattice gases: the variance grows sub-diffusively and in exactly the same way as in the absence of the external force, the same happens for the kurtosis, and only the skewness shows some dependence on βF.
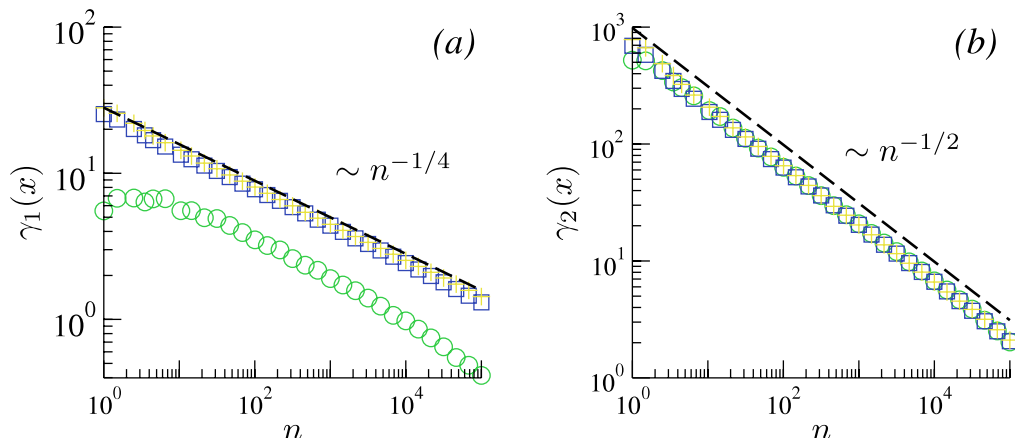
Figure 7. The skewness $\gamma_1(x)$ (panel (a)) and the kurtosis $\gamma_2(x)$ (panel (b)) of the probability distribution function of the displacement of a biased intruder in dense (with $\rho_0 = 0.002$) single-file lattice gases for different values of βF: $\beta F = 1$ ($\circ$), $\beta F = 5$ ($\square$) and $\beta F = 100$ ($+$). The dashed lines indicate the slopes $n^{-1/4}$ (panel (a)) and $n^{-1/2}$ (panel (b)).

6.2. Slit-like pores, stripes and capillaries

In this subsection we present a qualitative generalization of our results exact in $O(\rho_0)$ obtained for infinite two-dimensional systems over the cases of 3D slit pores ($L_x = L_y = \infty$ and L_z fixed), 2D stripes ($L_x = \infty$ and L_y fixed) and rectangular 3D capillaries ($L_x = \infty$, L_y and L_z fixed). First we focus on the time dependence of the variance of the biased intruder in the direction of the applied bias, building up our theoretical arguments on the structure of the result in equation (27). The latter can be represented as

$$\sigma_x^2 \sim \rho_0 \, a_1 \, n + \rho_0 \, a_0^2 \, \frac{n}{\chi_n}, \tag{33}$$

where a_0 and a_1 are (geometry-dependent) functions of βF, and χ_n is the mean number of new sites visited in the nth step by any of the vacancies. By definition, χ_n is given by [65]

$$\chi_n = S_n - S_{n-1}, \tag{34}$$

where S_n is a fundamental characteristic property of a lattice discrete-time random walk defining the mean number of *distinct* lattice sites visited by any of the vacancies up to time n. Its continuous-space and continuous-time counterpart, called in the mathematical literature the mean volume of the Wiener sausage, is the mean volume swept up to time t by a finite-sized diffusive particle (see, e.g., [75, 76, 79] and references therein).

In general, for systems which are *infinite* at least in one direction, the long-time asymptotical behaviour of S_n follows a power law of the form

$$S_n \sim n^\alpha, \tag{35}$$

where the exponent $\alpha \leq 1$ depends on the effective dimensionality of the lattice. In general (and not necessarily for standard Polya walks only), the exponent α is indicative of the degree of oversampling: larger α means that a vacancy returns less to already visited sites and mostly moves to new sites. In contrast, smaller α would indicate that a vacancy predominantly revisits already visited sites, so the spatial extent of its typical trajectory

would be smaller. In other words, α is an indicator of the degree of mixing of the lattice gas with larger values of α corresponding to a better mixing.

Note that $\alpha < 1$ for systems in which the random walk is recurrent, while equation (35) with $\alpha = 1$ holds for systems in which random walks are not recurrent. For its continuous counterpart, the mean volume of the Wiener sausage shows exactly the same power-law behaviour with $\alpha < 1$ for systems in which random (not necessarily standard Brownian) motion is, in the nomenclature of de Gennes [77], *compactly* exploring space, and $\alpha = 1$ corresponds to the case of the so-called non-compact exploration. Examples corresponding to the former and to the latter cases can be found in [75, 76, 79].

Noticing that, by virtue of equations (34) and (35), the mean number of new visited sites $\chi_n \sim n^{\alpha-1}$, supposing that $\alpha < 1$ (i.e., dealing with recurrent random walks or a random motion which compactly explores space), and assuming that equation (33) still holds, we infer that the leading long-time behaviour of the variance σ_x^2 is governed by the second term on the right-hand side of equation (33), and so

$$\sigma_x^2 \sim \rho_0 \, n^{2-\alpha}. \tag{36}$$

Capitalizing on the latter relation, we may draw an important qualitative conclusion: the smaller α is, i.e., the less efficient the mixing of the lattice gas by the vacancies is, the faster the growth of the variance of the BI displacement will be. For $\alpha = 1$, i.e., for non-recurrent random walks or non-compact exploration of space, in which case the mixing of the system by the vacancies is most efficient, both terms in equation (33) grow in proportion to time n, so the overall behaviour is diffusive.

Note that in the marginal case, i.e., for infinite two-dimensional systems, the leading long-time behaviour of the mean number of distinct sites visited follows (see, e.g., [65]) $S_n \sim \pi n / \ln(n)$, so $\chi_n \sim \pi / \ln(n)$ and we recover our exact result of equation (27).

We turn next to some specific confined geometries of interest. Suppose that we have a three-dimensional slit-like geometry characterized by $L_x = L_y = \infty$ and a fixed finite thickness L_z. For such a geometry one finds an effectively two-dimensional behaviour for the mean number of distinct sites visited, that is, $S_n \sim L_z n / \ln(n)$. This implies that the mean number of new sites visited in the nth step behaves asymptotically as $\chi_n \sim L_z / \ln(n)$ and consequently, the variance in the limit $n \to \infty$ obeys an asymptotic, weakly super-diffusive law

$$\sigma_x^2 \sim \frac{\rho_0}{L_z} \, n \, \ln(n), \tag{37}$$

which is similar to the exact result that we obtained for infinite two-dimensional systems.

For infinite two-dimensional stripes such that $L_x = \infty$ and L_y is fixed, one finds [72] $S_n \sim L_y n^{1/2}$, which implies that $\chi_n \sim L_y / n^{1/2}$, so the variance exhibits a strongly super-diffusive behaviour:

$$\sigma_x^2 \sim \frac{\rho_0}{L_y} \, n^{3/2}. \tag{38}$$

Lastly, for infinitely long rectangular capillaries with $L_x = \infty$ and L_y, L_z fixed, we have $S_n \sim L_y L_z n^{1/2}$ and $\chi_n \sim L_y L_z / n^{1/2}$, so

$$\sigma_x^2 \sim \frac{\rho_0}{L_y \, L_z} \, n^{3/2}, \tag{39}$$
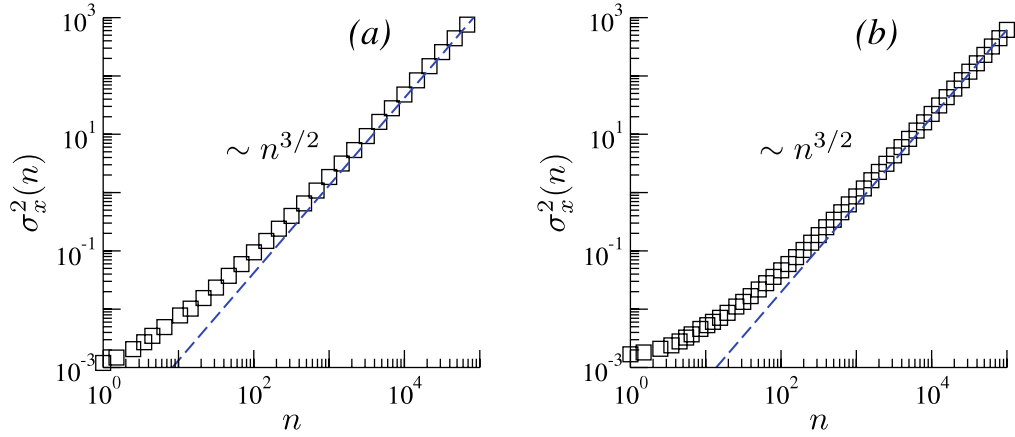
Figure 8. Monte Carlo simulation results for the variance σ_x^2 of the BI displacement in infinite stripes (panel (a)) and rectangular capillaries (panel (b)) for $\rho_0 = 0.002$ and $\beta F = 100$. The dashed lines in both panels have the slope $n^{3/2}$.

i.e., again a strongly super-diffusive behaviour is shown. Both equations (38) and (39) predict that the variance $\sigma_x^2 \sim n^{3/2}$ in the leading order in n, which is a straightforward consequence of the fact that both systems are effectively one-dimensional ones. Monte Carlo simulations performed for very elongated stripes ($L_x = 10^4$ and $L_y = 3$) and capillaries ($L_x = 10^4$ and $L_y = L_z = 3$)—see figure 8—confirm our predictions. Note that here, like for infinite 2D systems, an anomalous super-diffusive behaviour of the variance along the direction of the bias starts to develop at rather early times, at $n \approx 10^3$. For such times, the mean displacement of the BI amounts just to 0.5 times a lattice spacing for $\beta F = 10^2$ and $\rho_0 = 0.002$. This signifies that in our case, contrary to the cases for many physical systems in which an anomalous behaviour shows up only at very large times, the super-diffusive growth of the variance along the direction of the bias appears already in the earliest stages of the process and thus can be accessed within MD simulations. As a matter of fact, this is quite consistent with the numerical results of the MD simulations of a biased intruder in binary Yukawa liquids in [57, 59], which revealed a crossover to a super-diffusive behaviour at rather early times. The dynamical exponent $\xi \approx 1.5$ observed in [59] for an elongated, capillary-like geometry appears to be exactly equal to the value 3/2 which we predict here.

To close this section we remark that the arguments presented in this subsection can be readily generalized for continuous-space and continuous-time dynamics, by identifying vacancies present in the lattice gas with some elementary units of the free volume (see [68] and references therein) which are sufficiently large to allow for any individual particle motion due to a direct swapping of its position with any such units, rather than due to collective motion of all particles. Note that, of course, such a picture is plausible only in a certain density/temperature range. Note, as well, that the effective density of such units is much smaller than the available free volume which makes our analysis of the behaviour in O(ρ_0) appropriate. One finds then from [78] that for an infinitely long capillary of radius R with reflecting boundaries, the mean volume S_t visited by an elementary free volume performing a Brownian motion with diffusion coefficient D_f within time t follows

$S_t \sim R^2 \sqrt{D_f t}$, so the variance grows in proportion to $t^{3/2}$. Note that the variance appears to be inversely proportional to $\sqrt{D_f}$, which confirms the trend observed in equation (36): namely, the less effective the mixing of the system is (i.e., with progressively smaller values of D_f), the more pronounced the anomalous broadening of fluctuations in the BI dynamics will be. We note as well that the arguments presented are not limited to standard random walks or Brownian motion, and can be readily generalized for other types of random motion performed by particles or vacancies—and in particular, when due to particle–particle interactions the motion of the latter becomes anomalous and can be considered as continuous-time random walks with a broad distribution of pausing times [63]–[65], [80]. Lastly, we notice that such a picture predicts that in three dimensions (and higher), the growth of the variance σ_x^2 along the direction of the bias will show a usual diffusive growth, since $S_n \sim n$.

7. The CTRW picture revisited

As observed in MD simulations of a BI dynamics in binary Yukawa liquids in [57, 58] and in Lennard-Jones liquids in [61], any individual trajectory of the biased intruder shows a highly intermittent behaviour along the direction of the bias: the BI occasionally moves on a small random distance, but spends most of its time caged by other particles. Similarly, in our discrete-space and discrete-time model, the intruder stays still under a 'dynamic arrest' on some lattice sites, being blocked by the lattice gas particles, until any of the vacancies arrives at an adjacent site and releases it. Such a type of random motion does indeed resemble a typical behaviour of the so-called continuous-time random walk (see, e.g., [63]–[65] and references therein) characterized by a broad distribution of waiting times—time intervals between the consecutive jumps. This similarity prompted the authors of [61] to propose a phenomenological CTRW-type model, allowing them to conclude that the ultimate regime of growth of the variance σ_x^2 is diffusive. This section is designed to provide a deeper look into this picture, proposing an approach in which the distribution of the waiting times is not postulated *ad hoc*, but emerges naturally due to the dynamics of the vacancies.

We turn to the CTRW-type description proposed in [61] and represent X_n—an instantaneous position of the BI along the x-axis at time moment n—as

$$X_n = \sum_i^{N_n} (x + \delta x_i), \tag{40}$$

where N_n is a discrete random process which defines the number of jumps that the BI made, for a given realization of the process, within the time interval n. Furthermore, x is the average translation that the BI performs along the force direction during a single jump and δx_i is considered as the remaining translational length, which is a zero-mean, delta-correlated random variable such that $\mathbb{E}\{\delta x_i\} = 0$ and $\mathbb{E}\{\delta x_i \delta x_j\} \sim \delta_{i,j}$, where $\delta_{i,j}$ is the Kronecker delta and $\mathbb{E}\{\cdot\}$ denotes averaging with respect to different realizations of the process [61]. Note that we appropriately changed the notation used in [61] to make it closer to that used in our work and also use discrete time n in place of the continuous-time variable t. Straightforward calculations give then for the variance σ_x^2 of X_n the following,

quite general result:

$$\sigma_x^2 = \mathbb{E}\{x_i^2\}\,\mathbb{E}\{N_n\} + x^2\,\mathrm{Var}\,(N_n) \tag{41}$$

where $\mathbb{E}\{N_n\}$ is the mean number of jumps made by the BI within time interval n and $\mathrm{Var}(N_n)$ is the variance of N_n.

Presenting some *ad hoc* assumptions on the form of the distribution of N_n, which, in fact, do not rely on any microscopic dynamics, the authors of [61] concluded that $\mathbb{E}\{N_n\} \sim n$ and that $\mathrm{Var}\,(N_n)$ grows in proportion to n in the asymptotic regime, i.e., diffusively. According to [61], the overall predicted behaviour of the function σ_x^2 consists of two linear regimes with two different *constant* slopes; a smaller one at the early stages of the process and a somewhat larger one (by less than an order of magnitude) at the later stages. In [61] the regime interpolating between two diffusive ones was interpreted as a super-diffusion, but no theoretical interpretation has been provided. Recall, as well, that our results rule out any super-diffusive behaviour in infinite three-dimensional systems.

In the remaining part of our paper, focusing on the description of the BI dynamics in the $\mathrm{O}(\rho_0)$ limit in quasi-1D (stripes and capillaries), 2D and quasi-2D (slabs) systems within a somewhat simplified version of our model, we proceed to show that, as a matter of fact, the discrete random process N_n is linked to some stochastic process which exhibits long-range temporal correlations in such confined geometries and entails the super-diffusive growth of $\mathrm{Var}(N_n)$ in such systems. From the physical point of view, such correlations appear due to the fact that in confined geometries the random walks executed by the vacancies are recurrent, so that when a vacancy arrives at the location of the BI, it will persistently return to its location. The statistics of such returns dominates the long-time evolution of $\mathrm{Var}(N_n)$ in $\mathrm{O}(\rho_0)$.

A simplified version of our model is defined as follows: we suppose that the force acting on the BI is sufficiently large that when any vacancy arrives at the site adjacent to the current location of the BI in the direction of the bias, the BI instantaneously swaps its position with this vacancy, while backward jumps can be discarded. As in previous sections, we constrain our consideration to very dense systems and focus on the long-time behaviour in $\mathrm{O}(\rho_0)$. Finally, we turn to the frame of reference in which the origin is placed at the site adjacent to the BI in the direction of the applied bias and suppose that the motion of the BI itself can be neglected in the first approximation. Within such a simplified model we will calculate $\mathrm{Var}(N_n)$ exactly without resorting to any conjecture on the form of the distribution of N_n.

In such a simplified model, evidently, the number N_n of jumps that the BI has performed within time interval n is equal to the number of times the origin has been occupied by at least one vacancy, i.e.,

$$N_n = \sum_{k=1}^{n} \eta_k, \tag{42}$$

where η_k is a Boolean random variable such that $\eta_k = 1$ in the case where at time moment k the origin is occupied by at least one vacancy, and $\eta_k = 0$ otherwise. Note that a similar random variable has been studied previously in [81].

From equation (42) we straightforwardly find that the variance of N_n obeys (for $n \geq 2$)

$$\text{Var}(N_n) = \sum_{k=1}^{n} \mathbb{E}\{\eta_k\}(1 - \mathbb{E}\{\eta_k\}) + 2\sum_{k=1}^{n-1} \sum_{k'=k+1}^{n} C_{k,k'}, \tag{43}$$

where we made use of the evident relation $\eta_k^2 = \eta_k$ and $C_{k,k'}$ is the correlation function of the form

$$C_{k,k'} = \mathbb{E}\{\eta_k \eta_{k'}\} - \mathbb{E}\{\eta_k\}\mathbb{E}\{\eta_{k'}\}. \tag{44}$$

Suppose next that, as described in section 2, our lattice comprises K sites with M vacancies placed initially at random positions $\mathbf{Z}_0^{(m)}$, $m = 0, 1, \ldots, M$, and the position of the mth vacancy at time moment k, for a given realization of its trajectory, is denoted as $\mathbf{Z}_k^{(m)}$. Then, the indicator variable η_k can be written down explicitly as

$$\eta_k = 1 - \prod_{m=1}^{M} \left(1 - \delta\left(\mathbf{Z}_k^{(m)}\right)\right)$$

$$= \sum_{m=1}^{M} \delta\left(\mathbf{Z}_k^{(m)}\right) - \sum_{m,m'} \delta\left(\mathbf{Z}_k^{(m)}\right)\delta\left(\mathbf{Z}_k^{(m')}\right) + \cdots, \tag{45}$$

where $\delta\left(\mathbf{Z}_k^{(m)}\right)$ is an auxiliary Boolean variable—an indicator of the event that the mth vacancy is at the origin at time moment k; $\delta\left(\mathbf{Z}_k^{(m)}\right)$ equals 1 if $\mathbf{Z}_k^{(m)} = 0$ and equals 0 otherwise.

Averaging η_k in equation (45) over all possible trajectories and starting points of all M vacancies, we get, in the leading order in ρ_0,

$$\mathbb{E}\{\eta_k\} = \sum_{m=1}^{M} \mathbb{E}\left\{\delta\left(\mathbf{Z}_k^{(m)}\right)\right\} = \frac{M}{K}\sum_{\mathbf{Z}_0} \text{Prob}\left(0, k|\mathbf{Z}_0, 0\right) = \rho_0, \tag{46}$$

where $\text{Prob}(0, k|\mathbf{Z}_0, 0)$ is the probability[10] of finding a vacancy at the origin at time moment k given that it commenced its random walk at site $\mathbf{Z}_0$. The last equality in equation (46) is due to the fact that the sum over all starting points of this probability is 1, which is just the normalization condition. Note, as well, that the higher order terms in equation (45) have a higher order in ρ_0.

We turn next to the behaviour of the correlation function $C_{k,k'}$ in equation (44). The correlation function of the Boolean occupation variables is given, in $\text{O}(\rho_0)$, by

$$\mathbb{E}\{\eta_k \eta_{k'}\} = \sum_{m=1}^{M}\sum_{m'=1}^{M} \mathbb{E}\left\{\delta\left(\mathbf{Z}_k^{(m)}\right)\delta\left(\mathbf{Z}_{k'}^{(m')}\right)\right\}$$

$$= \sum_{m=1}^{M} \mathbb{E}\left\{\delta\left(\mathbf{Z}_k^{(m)}\right)\delta\left(\mathbf{Z}_{k'}^{(m)}\right)\right\} + 2\sum_{m=1}^{M-1}\sum_{m'=m+1}^{M} \mathbb{E}\left\{\delta\left(\mathbf{Z}_k^{(m)}\right)\right\}\mathbb{E}\left\{\delta\left(\mathbf{Z}_{k'}^{(m')}\right)\right\}$$

---

[10] We discard the effect of an instantaneous transition from the origin $X = 0$ to the site $X = -1$ due to the interaction with the BI and suppose that $\text{Prob}(0, k|\mathbf{Z}_0, 0)$ is that of a standard, unperturbed random walk [65].

$$= \frac{M}{K} \sum_{\mathbf{Z}_0} \mathrm{Prob}\,(0, k'|0, k|\mathbf{Z}_0, 0) + \frac{M(M-1)}{K^2}$$

$$= \rho_0 \, \mathrm{Prob}\,(0, k' - k|0, 0) + \rho_0^2, \tag{47}$$

where $\mathrm{Prob}\,(0, k'|0, k|\mathbf{Z}_0, 0)$ is the probability that a random walk starting at $\mathbf{Z}_0$ will arrive at the origin at the kth step, and will again revisit the origin at the k'th step, and $\mathrm{Prob}\,(0, k' - k|0, 0)$ is the probability that a random walk commencing at the origin will be at the origin at time moment $k' - k$. Noticing next that the term ρ_0^2 in the right-hand side of the latter equation cancels exactly with the term $-\overline{\eta_k}\,\overline{\eta_{k'}}$ in equation (44), we find that the correlation function $C_{k,k'}$ in $\mathrm{O}(\rho_0)$ is given by

$$C_{k,k'} = \rho_0 \, \mathrm{Prob}(0, k' - k|0, 0), \tag{48}$$

so, conveniently rearranging summations, we find eventually that the variance $\mathrm{Var}\,(N_n)$ of the number of jumps performed by the BI within time interval n obeys

$$\mathrm{Var}\,(N_n) \sim \rho_0 \, n + 2\,\rho_0 \sum_{p=1}^{n-1} \sum_{k=1}^{p} \mathrm{Prob}\,(0, k|0, 0). \tag{49}$$

The asymptotic behaviour of $\mathrm{Var}\,(N_n)$ in equation (49) can be readily defined by introducing the generating function $\mathrm{Var}\,(N_n)_z = \sum_{n=1}^{\infty} \mathrm{Var}\,(N_n)\, z^n$ and then analysing its leading singular behaviour in the limit $z \to 1^-$. Here we resort to a more straightforward but qualitative analysis of the behaviour of the second term on the right-hand side of equation (49), aiming just to determine its growth rate. To do this, note first that $\mathrm{Prob}\,(0, k|0, 0)$ is a monotonically decreasing function of the argument k and $\mathrm{Prob}\,(0, k|0, 0) \sim k^{-d/2}$ when $k \to \infty$, where d has to be understood as an effective spatial dimension of the system under study. Therefore, the correlation function in equation (48) decays *algebraically* in any spatial dimension and N_n in equation (42) is the sum of strongly *correlated* random variables.

Now, the asymptotic growth of the double sum on the right-hand side of equation (49) depends on how rapidly $\mathrm{Prob}\,(0, k|0, 0)$ decays with k, i.e., on the effective spatial dimension d. For $d = 1$, i.e., for quasi-1D systems, e.g., infinitely long stripes or infinitely long rectangular capillaries, $\mathrm{Prob}\,(0, k|0, 0) \sim 1/\sqrt{k}$, so the double sum in the right-hand side of equation (49) grows in proportion to $n^{3/2}$ and hence, by virtue of equation (41), we recover the super-diffusive behaviour discussed in the previous section. For $d = 2$, i.e., in two-dimensional cases and in quasi-three-dimensional slit pores, we have $\mathrm{Prob}\,(0, k|0, 0) \sim 1/k$, which results in the asymptotic law $\sim n \ln(n)$, obtained via a rigorous approach in section 4. Finally, for $d > 2$, one has a growth linear with time n of the second term in the right-hand side of equation (49) and, hence, an overall diffusive growth of the variance of the BI displacement along the direction of the bias. Note, however, that in three-dimensional systems these correlations provide an additional contribution to the effective diffusion coefficient. Note also that similar effects of correlations for random motion with compact/non-compact exploration of space have been discussed recently in [82].

To further elucidate the properties of the discrete random process, we turn to a zero-mean random process $\delta N_n = N_n - \mathbb{E}\{N_n\}$, which describes fluctuations of the number of jumps performed by the BI within time interval n, and focus on the correlation function of the form $\mathbb{E}\{(\delta N_n - \delta N_m)^2\}$ at two different time moments n and m, such that $n \geq m$.

25

Straightforward calculations give

$$\mathbb{E}\left\{(\delta N_n - \delta N_m)^2\right\} \sim \rho_0(n-m) + 2\,\rho_0 \sum_{p=1}^{(n-m)-1} \sum_{k=1}^{p} \mathrm{Prob}\left(0, k|0, 0\right), \qquad (50)$$

where the second term on the right-hand side is defined for $n > m + 1$ and equals 0, otherwise. This result is exact in $\mathrm{O}(\rho_0)$ and generalizes our equation (49).

The following points are to be emphasized. It is very likely, in view of our previous results, that the distribution of δN_n converges as $n \to \infty$ to a Gaussian distribution in any spatial dimension. Random process δN_n has stationary increments since the correlation function in equation (50) depends only on the difference $(n-m)$. In confined geometries, for $n \gg m$, the dominant behaviour of $\mathbb{E}\{(\delta N_n - \delta N_m)^2\}$ is given by the second, super-diffusive term, which entails $\mathbb{E}\{(\delta N_n - \delta N_m)^2\} \sim (n-m)^{3/2}$ for quasi-one-dimensional systems and $\mathbb{E}\{(\delta N_n - \delta N_m)^2\} \sim (n-m)\ln(n-m)$ for two-dimensional and quasi-two-dimensional systems, which signifies that the increments of the process δN_n are positively correlated. Summing up these three points, we may argue that the process δN_n behaves effectively as a super-diffusive fractional Brownian motion [70] with the Hurst index $H = 3/4$ for quasi-one-dimensional geometries and is weakly, logarithmically super-diffusive for 2D and quasi-2D geometries.

8. Conclusions

We have studied the dynamics of a hard-core intruder, biased by a constant external force F, in a quiescent medium modelled as a dense lattice gas of hard-core particles which move randomly without any preferential direction. From a different perspective, this system can be viewed as an asymmetric simple exclusion process (ASEP) evolving in a sea of symmetric exclusion processes (SEPs). It is well-known (see, e.g., [27]–[29]) that an essentially cooperative behaviour emerges in such a system such that the biased intruder (BI) drives the gas to a non-equilibrium steady state characterized by an inhomogeneous, asymmetric spatial distribution of particles, which attains a stationary form in the frame of reference moving with the intruder. In turn, the BI terminal velocity v depends, in a non-linear fashion, on the size of the inhomogeneities that it produces, on the value of the pulling force and on the density of the lattice gas particles. Here, looking beyond the usual analysis of the force–velocity relation, we obtained a number of new results in the leading order in the density of vacancies in the system, revealing an anomalous, field-induced behaviour of the higher moments of the BI displacement, and provided a physical explanation of the processes underlying the predicted behaviour. We emphasized the vacancy-controlled mechanism of fluctuation broadening in the dynamics of a biased intruder and highlighted the crucial role of the system's geometry: as a matter of fact, we showed that one can encounter a remarkably different behaviour in seemingly similar geometries, like single files versus quasi-1D systems (2D stripes or 3D capillaries), infinite 3D systems versus 3D slit-like pores. This anomalous behaviour may range from sub-diffusion to super-diffusion (see table 1).

For spatial dimension $d > 1$, an instantaneous position X_n at time n of the BI along the direction of the applied bias (along the x-axis) can be represented as $X_n = v\,n + \delta X_n$, where δX_n is a random variable with zero mean. Via an approach which is exact in

the lowest order in the density of vacancies, we have shown that despite this being such a non-equilibrium and non-homogeneous situation, for infinite two-dimensional systems the probability distribution of the random variable δX_n converges to a zero-mean Gaussian distribution as time $n \to \infty$. The first large-n correction term to the Gaussian distribution has also been determined, which enabled us to estimate the rate of convergence to the asymptotic behaviour. We have found that the variance σ_x^2 of this variable exhibits a weakly super-diffusive growth, $\sigma_x^2 \sim \nu_1 \, n \, \ln(n)$, where the coefficient ν_1 has been determined exactly for arbitrary bias in the lowest order in the density of vacancies in such a system. We have shown that $\nu_1 \sim F^2$ for small pulling forces F, which signifies that this weakly super-diffusive behaviour emerges beyond and thus cannot be derived within the linear-response approximation. It was shown that in the direction perpendicular to the bias (along the y-axis) the distribution of the BI displacement converges to a Gaussian but the variance σ_y^2 exhibits an effectively diffusive growth, $\sigma_y^2 \sim \nu_2 n$. The prefactor ν_2 has also been defined exactly, for arbitrary bias, in the lowest order in the density of vacancies.

Furthermore, capitalizing on our exact results for infinite two-dimensional systems, we have presented some qualitative arguments, based on the analysis of the structure of the exact results obtained, which allowed us to reproduce the behaviour obtained for infinite 2D systems in the leading order in the density of vacancies and to conjecture the behaviour of the variance σ_x^2 of the random variable δX_n in several quasi-one-dimensional geometries—infinitely long two-dimensional stripes and three-dimensional rectangular capillaries. We realized that in such confined geometries the field-induced broadening of fluctuations becomes much more pronounced and the variance shows a strongly super-diffusive behaviour, $\sigma_x^2 \sim n^{3/2}$. Our analytical predictions are confirmed by Monte Carlo simulations.

Pursuing our analysis further, we revisited a CTRW-like picture proposed previously in [61]. We have shown that from the mathematical point of view, the super-diffusive broadening of fluctuations of the BI trajectories in confined geometries arises due to the fact that the key property in the CTRW picture—the discrete random process N_n describing the number of jumps made by the BI during time interval n—appears to be linked to a hidden random process, which behaves asymptotically as a super-diffusive fractional Brownian motion (fBm) [70] with the Hurst index $H = 3/4$ for quasi-one-dimensional geometries and contains an additional logarithmic factor for two-dimensional and quasi-two-dimensional systems. In these situations, this process governs the long-time behaviour of the variance of N_n in $O(\rho_0)$. From the physical point of view, the mechanism underlying this super-diffusive fBm-type process emerging in confined geometries is associated with persistent recurrent returns to the BI location of the vacancies which have interacted once with the BI. Therefore, we argued that the BI dynamics represents a rather interesting combination of two different kinds of stochastic processes—CTRW-type and fBm-type processes.

Finally, we have presented the results of Monte Carlo simulations of the dynamics of a biased intruder in a strictly one-dimensional lattice gas of unbiased hard-core particles, i.e., in the so-called single-file lattice gas. We have shown that the variance σ_x^2 of the random variable δX_n (defined now via $X_n = \nu \sqrt{n} + \delta X_n$) grows in proportion to $\sqrt{n}$, precisely in the way that it does in the case of an unbiased intruder. Moreover, we demonstrated that even the prefactor in this growth law appears to be independent of the

magnitude of the external bias. Also, we have shown that the kurtosis of the distribution of δX_n vanishes as $n \to \infty$, which signifies that this distribution becomes Gaussian in the long-time limit. Analytical analysis of the biased diffusion in single-file lattice gas will be presented elsewhere [69].

Acknowledgment

References

[1] Gutsche C, Kremer F, Krüger M, Rauscher M, Weeber R and Harting J, 2008 *J. Chem. Phys.* **129** 084902
[2] Pesic J, Terdik J Z, Xu X, Tian Y, Lopez A, Rice S A, Dinner A R and Scherer N F, 2012 *Phys. Rev.* E **86** 031403
[3] Candelier R and Dauchot O, 2010 *Phys. Rev.* E **81** 011304
[4] Krüger M and Rauscher M, 2009 *J. Chem. Phys.* **131** 094902
[5] Ladadwa I and Heuer A, 2013 *Phys. Rev.* E **87** 012302
[6] Reichhardt C and Olson Reichhardt C J, 2004 *Phys. Rev. Lett.* **92** 108301
[7] Dzubiella J, Löwen H and Likos C N, 2003 *Phys. Rev. Lett.* **91** 248301
[8] Krüger M and Rauscher M, 2007 *J. Chem. Phys.* **127** 034905
[9] Mejía-Monasterio C and Oshanin G, 2011 *Soft Matter* **7** 993
[10] Pacheco-Vázquez F and Ruiz-Suárez J C, 2010 *Nat. Commun.* **1** 123
[11] Kliushnychenko O V and Lukyanets S P, 2013 *Eur. Phys. J. Special Topics* **216** 127
[12] Hastings M, Olson Reichhardt C and Reichhardt C, 2003 *Phys. Rev. Lett.* **90** 98302
[13] Habdas A, Schaar D, Levitt A and Weeks E, 2004 *Europhys. Lett.* **67** 477
[14] Gazuz I, Puertas A, Voigtmann T and Fuchs M, 2009 *Phys. Rev. Lett.* **102** 248302
[15] Zik O, Stavans J and Rabin Y, 1992 *Europhys. Lett.* **17** 315
[16] Sarracino A, Villamaina D, Gradenigo G and Puglisi A, 2010 *Europhys. Lett.* **92** 34001
[17] Olson Reichhardt C J and Reichhardt C, 2010 *Phys. Rev.* E **82** 051306
[18] Fiege A, Grob M and Zippelius A, 2012 *Granular Matter* **14** 247
[19] Gradenigo G, Puglisi A, Sarracino A, Villamaina D and Vulpiani A, *Out-of-equilibrium generalized fluctuation-dissipation relations*, 2012 *Non-Equilibrium Statistical Physics of Small Systems: Fluctuation Relations and Beyond* ed R Klages, W Just and C Jarzynski (Weinheim: Wiley-VCH)
[20] Démery V and Dean D S, 2010 *Phys. Rev. Lett.* **104** 080601
[21] Dean D S and Démery V, 2011 *J. Phys.: Condens. Matter* **23** 234114
[22] Démery V and Dean D S, 2011 *Phys. Rev.* E **84** 010103
[23] Burlatsky S F, Oshanin G, Mogutov A and Moreau M, 1992 *Phys. Lett.* A **166** 230
[24] Burlatsky S F, Oshanin G, Moreau M and Reinhardt W P, 1996 *Phys. Rev. E* **54** 3165
[25] Landim C, Olla S and Volchan S B, 1998 *Commun. Math. Phys.* **192** 287
[26] Oshanin G, Bénichou O, Burlatsky S F and Moreau M, *Biased tracer diffusion in hard-core lattice gases: some notes on the validity of the Einstein relation*, 2004 *Instabilities and Nonequilibrium Structures IX* ed O Descalzi, J Martinez and S Rica (Dordrecht: Springer) pp 33–74
[27] De Coninck J, Oshanin G and Moreau M, 1997 *Europhys. Lett.* **38** 527
[28] Bénichou O, Cazabat A M, De Coninck J, Moreau M and Oshanin G, 2000 *Phys. Rev. Lett.* **84** 511
    Bénichou O, Cazabat A M, De Coninck J, Moreau M and Oshanin G, 2001 *Phys. Rev. B* **63** 235413
[29] Bénichou O, Cazabat A M, Moreau M and Oshanin G, 1999 *Physica A* **272** 56
    Bénichou O, Klafter J, Moreau M and Oshanin G, 2000 *Phys. Rev. E* **62** 3327

[30] Chou T, Mallick K and Zia R K P, 2011 *Rep. Prog. Phys.* **74** 116601
[31] Spohn H, 1991 *Large Scale Dynamics of Interacting Particles* (Berlin: Springer)
[32] Kehr K and Binder K, *Simulations of diffusion in lattice gases and related kinetic phenomena*, 1984 *Applications of the Monte Carlo Methods in Statistical Physics* ed K Binder (Berlin: Springer) p 181
[33] Kob W and Andersen H C, 1993 *Phys. Rev. E* **48** 4364
[34] Kurchan J, Peliti L and Sellitto M, 1997 *Europhys. Lett.* **39** 365
[35] Imparato A and Peliti L, 2000 *Phys. Lett.* A **269** 154
[36] Toninelli C, Biroli G and Fisher D S, 2004 *Phys. Rev. Lett.* **92** 185504
[37] Jack R L, Kelsey D, Garrahan J P and Chandler D, 2008 *Phys. Rev. E* **78** 011506
[38] Sellitto M and Arenzon J J, 2000 *Phys. Rev. E* **62** 7793
[39] Corberi F and Cugliandolo L F, 2009 *J. Stat. Mech.* P09015
[40] Ritort F and Sollich P, 2003 *Adv. Phys.* **52** 219
[41] Imparato A and Peliti L, 2007 *J. Stat. Mech.* L02001
[42] Golubeva N and Imparato A, 2012 *Phys. Rev. Lett.* **109** 190602
[43] Burlatsky S F, Oshanin G, Cazabat A M and Moreau M, 1996 *Phys. Rev. Lett.* **76** 86
Burlatsky S F, Oshanin G, Cazabat A M, Moreau M and Reinhardt W P, 1996 *Phys. Rev. E* **54** 3832
[44] Popescu M N, Oshanin G, Dietrich S and Cazabat A M, 2012 *J. Phys.: Condens. Matter* **24** 243102
[45] Oshanin G, De Coninck J, Cazabat A M and Moreau M, 1998 *Phys. Rev. E* **58** R20
Oshanin G, De Coninck J, Cazabat A M and Moreau M, 1998 *J. Mol. Liquids* **76** 195
[46] Antal T, Krapivsky P L and Redner S, 2009 *J. Theor. Biol.* **261** 488
[47] Ferrari P, Goldstein S and Lebowitz J L, *Diffusion, mobility and the Einstein relation*, 1985 *Statistical Physics and Dynamical Systems* ed J Fritz, A Jaffe and D Szasz (Boston: Birkhauser) p 405
[48] Gradenigo G, Puglisi A, Sarracino A, Vulpiani A and Villamaina D, 2012 *Phys. Scr.* **86** 058516
[49] Harris T E, 1965 *J. Appl. Probab.* **2** 323
[50] Levitt D G, 1973 *Phys. Rev. A* **8** 3050
[51] Spitzer F, 1970 *Adv. Math.* **5** 246
[52] Fedders P A, 1978 *Phys. Rev. B* **17** 40
[53] Alexander S and Pincus P, 1978 *Phys. Rev. B* **18** 2011
[54] Arratia R, 1983 *Ann. Probab.* **11** 362
[55] Wei Q -H, Bechinger C and Leiderer P, 2000 *Science* **287** 625
[56] Lutz C, Kollmann M and Bechinger C, 2004 *Phys. Rev. Lett.* **93** 026001
[57] Winter D, Horbach J, Virnau P and Binder K, 2012 *Phys. Rev. Lett.* **108** 028303
[58] Winter D and Horbach J, 2013 *J. Chem. Phys.* **138** 12A512
[59] Harrer Ch J, Winter D, Horbach J, Fuchs M and Voigtmann Th, 2012 *J. Phys.: Condens. Matter* **24** 464105
[60] Bénichou O, Mejía-Monasterio C and Oshanin G, 2013 *Phys. Rev. E* **87** 020103
[61] Schroer C F E and Heuer A, 2013 *Phys. Rev. Lett.* **110** 067801
[62] Bouchaud J P *et al,* 1990 *Ann. Phys.* **201** 285
[63] Metzler R and Klafter J, 2000 *Phys. Rep.* **339** 1
[64] Metzler R and Klafter J, 2004 *J. Phys. A: Math. Gen.* **37** R161
[65] Hughes B D, 1995 *Random Walks and Random Environments* (Oxford: Oxford Science Publishers)
[66] Cugliandolo L F, 2011 *J. Phys. A: Math. Theor.* **44** 483001
[67] Seifert U, 2012 *Rep. Prog. Phys.* **75** 126001
[68] Widmer-Cooper A and Harrowell P, 2005 *J. Phys.: Condens. Matter* **17** S4025
[69] Illien P, Bénichou O, Mejia-Monasterio C, Oshanin G and Voituriez R, in preparation
[70] Mandelbrot B B and van Ness J W, 1968 *SIAM Rev.* **10** 422
[71] Bénichou O and Oshanin G, 2002 *Phys. Rev. E* **66** 031101
Bénichou O and Oshanin G, 2001 *Phys. Rev. E* **64** 020103
[72] Brummelhuis M J A M and Hilhorst H J, 1989 *Physica A* **156** 575
[73] Nakazato K and Kitahara K, 1980 *Prog. Theor. Phys.* **64** 2261
[74] van Beijeren H and Kutner R, 1985 *Phys. Rev. Lett.* **55** 238
[75] Oshanin G, Moreau M and Burlatsky S F, 1994 *Adv. Colloid Interface Sci.* **49** 1
[76] Bénichou O, Moreau M and Oshanin G, 2000 *Phys. Rev.* E **61** 3388
[77] de Gennes P G, 1982 *J. Chem. Phys.* **76** 3316
de Gennes P G, 1982 *J. Chem. Phys.* **76** 3322
[78] Dagdug L and Berezhkovskii A M, 2006 *J. Chem. Phys.* **125** 244705
[79] Burlatsky S F and Oshanin G, 1990 *Phys. Lett. A* **145** 61
Oshanin G and Burlatsky S F, 1991 *J. Stat. Phys.* **65** 1109
[80] Franke J and Majumdar S N, 2012 *J. Stat. Mech.* P05024
[81] Boguna M, Berezhkovskii A M and Weiss G H, 2000 *Phys. Rev. E* **62** 3250
[82] Meyer B, Bénichou O, Kafri Y and Voituriez R, 2012 *Biophys. J.* **102** 2186